(Preprint) AAS XX-XXX

REMEDIATING NON-POSITIVE DEFINITE STATE COVARIANCES FOR COLLISION PROBABILITY ESTIMATION

Doyle T. Hall,[*] Matthew D. Hejduk,[†] and Lauren C. Johnson[‡]

The NASA Conjunction Assessment Risk Analysis team estimates the probability of collision (P_c) for a set of Earth-orbiting satellites. The P_c estimation software processes satellite position+velocity states and their associated covariance matrices. On occasion, the software encounters *non-positive definite* (NPD) state covariances, which can adversely affect or prevent the P_c estimation process. Interpolation inaccuracies appear to account for the majority of such covariances, although other mechanisms contribute also. This paper investigates the origin of NPD state covariance matrices, three different methods for remediating these covariances when and if necessary, and the associated effects on the P_c estimation process.

INTRODUCTION

The NASA Conjunction Assessment Risk Analysis (CARA) team estimates the probability of collision (P_c) for a specific set of high-value Earth-orbiting satellites. For each conjunction, the CARA software system calculates P_c using inertial-frame position+velocity states and associated covariance matrices for both the primary and secondary satellites, specified at the time of closest approach (TCA). Orbit determination (OD) processes[1] typically provide positive definite (PD) covariances, or at least positive semi-definite (PSD) covariance matrices – characterized by real eigenvalues that are all > 0 or ≥ 0, respectively. On occasion, however, the CARA system encounters non-positive definite (NPD) state covariances – most often characterized by one slightly negative eigenvalue.

NPD covariances can conceivably arise in a variety of ways. For instance, interpolating from an ephemeris of covariances to obtain TCA estimates can introduce inaccuracies that yield NPD matrices.[2] Inaccuracies can also be introduced when converting from one state representation system to another (such as between orbital elements and inertial state vectors) using first-order or finite-difference transformation approximations. Computational precision limitations can similarly create NPD covariances, even when performing otherwise exact transformations (such as basis-vector rotations). NPD matrices can also arise from truncation errors that occur when numerically storing or transmitting covariances using data structures with a limited bit length or number of significant figures. Preliminary analysis indicates that interpolation inaccuracies account for the majority of NPD covariances currently encountered by the CARA system, although other mechanisms may contribute as well.

[*] Senior CARA Analyst, Omitron Inc., 555 E. Pikes Peak Ave, #205 Colorado Springs, CO 80903.
[†] Chief Engineer, NASA Robotic CARA, Astrorum Consulting LLC, 10006 Willow Bend Dr, Woodway, TX 76712.
[‡] CARA Analysis Team Lead, Omitron Inc., 555 E. Pikes Peak Ave, #205 Colorado Springs, CO 80903.

From a purely computational point of view, P_c estimation processes do not always require fully PD state covariance matrices for both of the objects involved in a conjunction. For instance, when the primary and secondary state covariances are uncorrelated, P_c values can be estimated using only their joint or summed covariances.[3] The CARA system occasionally processes conjunctions that have an NPD primary or secondary state covariance, but when summed yield a PD joint covariance matrix – a situation that raises concern but does not actually prevent the P_c computation. Similarly, the often-used "2D P_c" approximation[3,4] only requires PD status for a marginalized, 2×2 relative position covariance at TCA, regardless of the status of the original state covariances. Finally, Monte Carlo (MC) methods[5] require repetitively sampling state probability distribution functions (PDFs) for both the primary and secondary objects, but these sampling computations only require PSD covariances.

Despite these situations, the CARA system does sometimes encounter conjunctions in which NPD covariances prevent the computation of P_c estimates or related quantities. For these situations, CARA's current approach is to "repair" the matrix as required for the specific calculation at hand. CARA has investigated three remediation methods for this task: *Spectrum Shifting* entails adding a small offset to the entire set of covariance eigenvalues, and then reconstructing a remediated covariance matrix using the original eigenvectors. *Higham Remediation*[6] employs a method developed for the financial industry to remediate NPD correlation matrices, by finding the closest PSD matrix in terms of Frobenius norm. This approach requires that the covariance first be transformed into a correlation matrix, which has the advantages of being dimensionless and often better conditioned than the original covariance. Finally, *Eigenvalue Clipping* sets a minimum limit for the eigenvalues of the covariance or correlation matrix, and simply forces smaller eigenvalues to this limit. There are different ways of establishing the eigenvalue limit. For instance, remediating NPD position covariances can employ physics-based considerations, specifically by using a clipping limit based on the precision of the original OD metric observations, or alternatively, a limit that corresponds to a small percentage of the satellite's hard-body radius.

This paper investigates the frequency that NPD covariance matrices occur by analyzing a large number of conjunctions archived in CARA's database, as well as describing three different methods for remediating these covariances when and if necessary, and the associated effects on the P_c estimation process.

ANALYSIS OF ARCHIVED CONJUNCTIONS

This section describes the analysis of actual conjunctions contained in CARA's data archive, to determine the frequency and circumstances in which improper NPD covariances occur.

Conjunction Data Supplied to CARA

Most conjunctions represent single, isolated close approach events between two satellites. These occur when the magnitude of the relative position vector, $|\mathbf{r}(t)|$, reaches a minimum in time. The U.S. Air Force maintains orbital states for a large catalog of trackable satellites, enabling predictions of such close approaches for CARA's set of high-value primary satellites.[7] Conjunction analysis occurs when any cataloged secondary satellite is predicted to make an incursion into a predefined screening volume centered on a primary.[7,8] For each conjunction, the CARA system receives and processes raw data similar to that contained in a standard conjunction data message (CDM) — produced in a previous and separate analysis. For purposes of this paper, the input data will be referred to hereafter as a CDM. Each CDM contains the time of close approach (t_{ca} or TCA), and many other quantities related to the orbital states and associated uncertainties of the primary and secondary objects for the conjunction.

ECI Frame Satellite States and Covariances

For instance, the CDM contains data that can be readily converted to the Earth-centered inertial (ECI) reference frame[9] mean position+velocity states for both the primary and secondary, $\mathbf{x}_p(t_{ca})$ and $\mathbf{x}_s(t_{ca})$, respectively, where $\mathbf{x}(t) = [\mathbf{r}(t)\ \mathbf{v}(t)]$. CDM's also contain state covariance data, originally expressed in the Cartesian *radial, in-track* and *cross-track* (RIC) reference frame[9] (also sometimes called the UVW frame). The RIC covariance matrices can be transformed to the ECI state covariances[9,10] for the primary and secondary, denoted here as $\mathbf{C}_p(t_{ca})$ and $\mathbf{C}_s(t_{ca})$, respectively, which have matrix dimensions of 6×6. These transformed quantities can then be used to define the relative ECI state at close approach, $\mathbf{x}(t_{ca}) = \mathbf{x}_s(t_{ca}) - \mathbf{x}_p(t_{ca})$, and the associated combined covariance $\mathbf{C}(t_{ca}) = \mathbf{C}_s(t_{ca}) + \mathbf{C}_p(t_{ca})$. The CARA software system employs TCA ECI states and covariances to estimate collision probabilities.

Marginalized Position and Velocity Covariances

The 6×6 ECI covariance matrices discussed can be decomposed into three 3×3 sub-matrices as follows

$$\mathbf{C} = \begin{bmatrix} \mathbf{A} & \mathbf{B}^T \\ \mathbf{B} & \mathbf{E} \end{bmatrix} \tag{1}$$

where **A** denotes the marginalized position-position covariance, **E** the marginalized velocity-velocity covariance, and **B** contains the position-velocity cross covariance terms. This report denotes covariance matrices and sub-matrices using all upper case letter symbols.

Correlation Matrices

Under most circumstances state covariances can be transformed into correlation matrices, denoted here using lower case symbols. These have unit diagonals, and can be calculated as follows: the correlation matrix, **c**, associated with covariance matrix, **C**, is given by[11]

$$\mathbf{c} = \mathbf{DCD} \tag{2}$$

where **D** denotes a diagonal matrix with elements $D_{i,j} = \delta_{i,j}\ (C_{i,i})^{-1/2}$, and $\delta_{i,j}$ denotes the Kronecker delta function. This conversion yields a proper, unit-diagonal correlation matrix only if all of the diagonal elements, $C_{i,i}$, are positive, which may not be true for an approximated covariance. In conjunction analysis, correlation matrices have the advantages of being dimensionless, and also usually much better conditioned than the original covariance. For instance, a 6×6 ECI state covariance, as given in equation (1), has elements with dimensions of m^2 in the **A** submatrix, $m^2\ s^{-2}$ in the **E** submatrix, and $m^2\ s^{-1}$ in the **B** submatrix. The six eigenvalues of such a mixed-dimension covariance are difficult to interpret physically, and can also span a much larger numerical range than those for the associated correlation matrix. Matrix condition numbers (calculated using the *cond* function of the Matlab software system) for the ECI state covariances $\mathbf{C}_p(t_{ca})$ and $\mathbf{C}_s(t_{ca})$ were found to have typical values of order $\sim 3\times10^{13}$ in the archive analysis, but condition numbers for the associated correlations matrices $\mathbf{c}_p(t_{ca})$ and $\mathbf{c}_s(t_{ca})$ were $\sim 3\times10^{7}$, six orders of magnitude smaller. The marginalized position covariances $\mathbf{A}_p(t_{ca})$ and $\mathbf{A}_s(t_{ca})$, had significantly better typical condition numbers of $\sim 3\times10^{3}$, and their correlation matrices $\mathbf{a}_p(t_{ca})$ and $\mathbf{a}_s(t_{ca})$ had even better condition numbers $\sim 10^{3}$.

Equinoctial Element States and Covariances

The ECI states and covariances for the primary and secondary objects can also be converted to equinoctial element mean states and covariances[9,10] denoted here using the primed symbols $\mathbf{x}'_k(t_{ca})$ and $\mathbf{C}'_k(t_{ca})$, respectively, where k represents either p or s. For this study, the Jacobian matrices required for ECI↔equinoctial covariance transformations were calculated numerically using a finite differencing algorithm. The equinoctial state covariances were found to be somewhat better conditioned than their associated ECI state covariances, with condition numbers typically factors of about 10 to 20 smaller. Equinoctial state correlation matrices were found to be the best conditioned among all of the 6×6 matrices analyzed here, with typical condition numbers ~3×10^2.

NPD Number and Status Indicators

Properly formulated and constructed covariance and correlation matrices cannot be NPD.[2,6,11] Trying to use NPD matrices without any remediation to calculate P_c values could prevent the calculation or potentially lead to inaccurate results. To prevent this, such NPD matrices must first be detected, and this section defines two indicators designed for this task. The first indicator of the NPD status of an $N\times N$ covariance matrix, $\mathbf{C}$, is given by the *NPD number*, $n(\mathbf{C})$, an integer quantity defined as the summed number of nonpositive eigenvalues. (All eigenvalues in this analysis were calculated using Matlab's *eig* function.) PD covariances have $n(\mathbf{C}) = 0$, and NPD covariances have $0 < n(\mathbf{C}) \le N$. The second indicator is the *NPD status*, $b(\mathbf{C}) = \min[1, n(\mathbf{C})]$, a binary quantity defined so that PD matrices have $b(\mathbf{C}) = 0$, and NPD matrices have $b(\mathbf{C}) = 1$.

The NPD number indicator for a correlation matrix, $\mathbf{c}$, can be defined similarly, except in the rare cases in which the original $N\times N$ covariance matrix, $\mathbf{C}$, has one or more diagonal elements less than or equal to zero. As explained above, this prevents the calculation of a proper, unit-diagonal correlation matrix. In these cases, the NPD number indicator is defined as $n(\mathbf{c}) = N+L$, where L is the number of nonpositive diagonal elements of $\mathbf{C}$. Defined this way, PD correlation matrices have $n(\mathbf{c}) = 0$, NPD correlations have $0 < n(\mathbf{c}) \le N$, and, in cases where proper correlations cannot be calculated, $N < n(\mathbf{c}) \le 2N$. The binary NPD status indicator for correlation matrices remains defined as $b(\mathbf{c}) = \min[1, n(\mathbf{c})]$.

NPD Fractions

The NPD analysis for a large, archived set of conjunctions can be conveniently summarized in the form of *NPD fractions*, which indicate the fraction of conjunctions involving an NPD matrix. For instance, for a set of M conjunctions, the fraction that have NPD primary object ECI state 6×6 covariances can be expressed as $F_p = \{\Sigma_m[b(\mathbf{C}_{m,p})]\} / M$, where Σ_m represents a summation over the set of M conjunctions, and $\mathbf{C}_{m,p}$ is the primary's ECI state covariance at TCA for the m^{th} archived conjunction. Likewise the NPD fraction for ECI relative state correlations is $f = \{\Sigma_m[b(\mathbf{c}_m)]\} / M$. The NPD fractions $\{F_p, f_p, F_s, f_s, F, f, F'_p, f'_p, F'_s, f'_s\}$ can all be defined similarly (again with upper-case symbols corresponding to covariances, lower-case to correlations, unprimed quantities to ECI states, primed quantities to equinoctial states, $\{p,s\}$ subscripts to primary and secondary object states, and no subscripts to relative states).

NPD Analysis of Two Years of Archived Conjunction Data

This study reports the analysis of 839,383 conjunctions that occurred during a 2-year period between 2015-04-01 and 2017-04-06. Of these, 8,874 were eliminated due to primary or secondary ECI state covariance matrices that contained all zeros, or that defined implausibly large 1-sigma position uncertainties greatly exceeding one earth radius. NPD number and status indicators, as defined above, were calculated for all of the remaining M = 830,509 conjunctions. Specifically, these indicators were calculated for the 6×6 ECI and equinoctial state covariance and correlation

matrices, as well as the 3×3 ECI position covariance and correlation matrices, and then used to calculate NPD fractions.

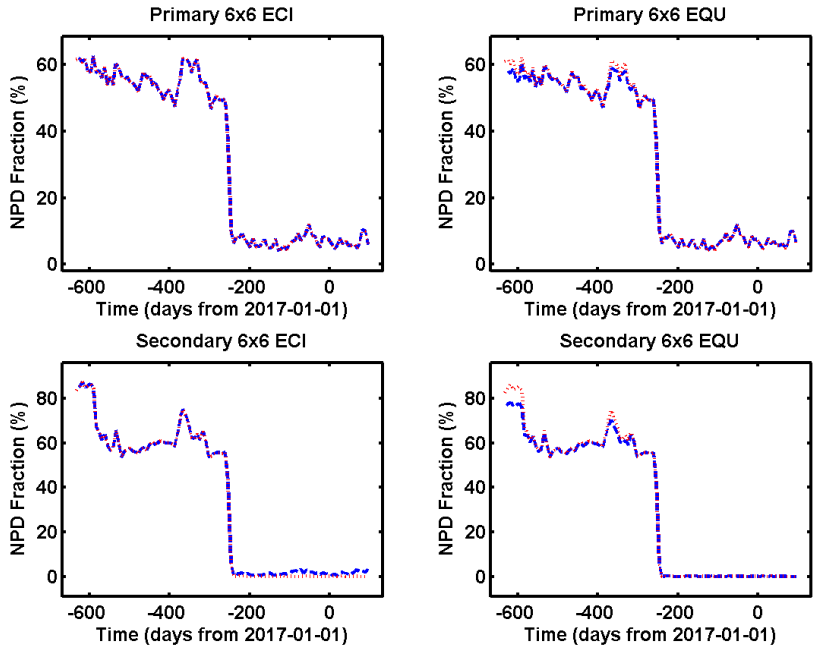

Figure 1. NPD fractions plotted as a function of time during the 2-year study period.

Figure 1 shows the NPD fractions for 6×6 state matrices $\{F_p, f_p, F_s, f_s, F'_p, f'_p, F'_s, f'_s\}$ plotted as a function of time during the 2-year study period using 1-week time bins. In Figure 1, the dashed blue lines correspond to covariance matrices and the dotted red lines to correlation matrices; the left-side panels to ECI states and the right panels to equinoctial states. Specifically, the top left panel of Figure 1 shows NPD fractions for the primary ECI state matrices (F_p dashed blue, f_p dotted red); the bottom left for secondary ECI matrices (F_s dashed blue, f_s dotted red); top right for primary equinoctial state matrices (F'_p dashed blue, f'_p dotted red); and bottom right for secondary equinoctial state matrices (F'_s dashed blue, f'_s dotted red). The corresponding NPD fractions for the 3×3 position matrices are all significantly smaller, and are not plotted here; in fact, the fractions $\{F_p, f_p, F'_p, f'_p\}$ were all found to be zero, except for one primary which had a small number of NPD occurrences (as discussed further below).

Notably, Figure 1 indicates that NPD fractions observed during the first 13 months of the 2-year study period were significantly larger than during the last 11 months, with a dramatic and sudden decrease occurring just before 2016-05-01. This improvement occurred because, near this time, the number of significant figures used to express RIC covariance elements within the CDMs expanded from 4 up to 16 — an increased precision that markedly reduced the number of NPD 6×6 matrices. This demonstrates explicitly that NPD matrices can arise when numerically storing or transmitting covariances using data structures with a limited precision due to a limited number of significant figures or bit length.

Because the earlier, lower precision data does not provide a good representation for future conjunctions, the remainder of the archive analysis concentrates on the later 11-month period.

NPD Analysis of High-Precision Archived Conjunction Data

A total of 433,768 conjunctions occurred during the 11-month period between 2016-05-01 and 2017-04-06. Of these, 5,179 were eliminated, as before, due to all-zero covariances or implausibly large position uncertainties. The remaining M = 428,589 conjunctions comprised 81 unique primary satellites, and occurred at a rate of about 8,000 per week. Again, NPD number and status indicators were calculated for all of these conjunctions. Table 1 along with Figures 2 and 3 summarize the results in the form of the NPD fractions $\{F_p, f_p, F_s, f_s, F'_p, f'_p, F'_s, f'_s\}$, as described earlier.

Table 1. NPD fractions for conjunction covariance and correlation matrices (%).

Number Of Primaries	Num. of Events M	*NPD Fractions (%) for 6x6 State Covariances (F) and Correlations (f)*									
		Cartesian ECI States						*Equinoctial States*			
		F_p	f_p	F_s	f_s	F	f	F'_p	f'_p	F'_s	f'_s
All 81	428589	6.81	6.76	1.62	0.20	0.12	0.06	6.76	6.76	0.20	0.20
72 with $e_p \le 0.01$	308971	8.4e-2	4.1e-2	1.36	0.14	8.4e-2	2.0e-2	4.1e-2	4.1e-2	0.14	0.14
9 with $e_p \ge 0.68$	119618	24.19	24.12	2.28	0.36	0.20	0.17	24.12	24.12	0.36	0.36
		NPD Fractions (%) for 3x3 Position Covariances (F) and Correlations (f)									
All 81	428589	6.8e-3	6.8e-3	1.2e-3	1.2e-3	1.9e-3	1.9e-3	NA*	NA	NA	NA
72 with $e_p \le 10^{-2}$	308971	0	0	6.5e-4	6.5e-4	6.5e-4	6.5e-4	NA	NA	NA	NA
9 with $e_p \ge 0.68$	119618	2.4e-2	2.4e-2	2.5e-3	2.5e-3	5.0e-3	5.0e-3	NA	NA	NA	NA

*NA = Not applicable; 3×3 marginalized matrices are only analyzed for Cartesian states.

The top part of Table 1 lists the results for analyses of 6×6 state matrices, and the bottom part summarizes the results for the marginalized 3×3 ECI position matrices. Among the 81 primary satellites, 72 were found to have low eccentricity orbits, with $e_p \le 10^{-2}$; the remaining 9 had very eccentric orbits, with $0.68 \le e_p \le 0.84$. A total of 29,201 of the 428,589 ECI primary state 6×6 covariances were found to be NPD, representing a fraction of F_p = 6.81%, as listed in the top data row of Table 1. The fraction of NPD primary ECI correlation matrices was slightly smaller at f_p = 6.76%, listed adjacently. The bottom part of Table 1 lists the NPD fractions for the marginalized 3×3 ECI position covariances and correlations $\{\mathbf{A}_{m,p}, \mathbf{a}_{m,p}, \mathbf{A}_{m,s}, \mathbf{a}_{m,p}, \mathbf{A}_m, \mathbf{a}_m\}$, which are significantly smaller than the NPD fractions for the 6×6 matrices (as discussed further below).

Figures 2 and 3 show NPD fractions for the 6×6 state matrices plotted as a function of time during the 11-month study period. Figure 2 shows the fractions for both primary and secondary objects for all of the conjunctions combined, in the same format used in Figure 1 above. Figure 3 separates the fractions for the primaries into low- and high-eccentricity groups. Specifically, the top panels of Figure 3 show NPD fractions for the 72 primaries with $e_p \le 10^{-2}$, and the bottom panels for the 9 other primaries with $0.68 \le e_p \le 0.84$. Again, the corresponding NPD fractions for the 3×3 position matrices are all zero, except for one primary (as discussed further in the next section), and are not plotted here.

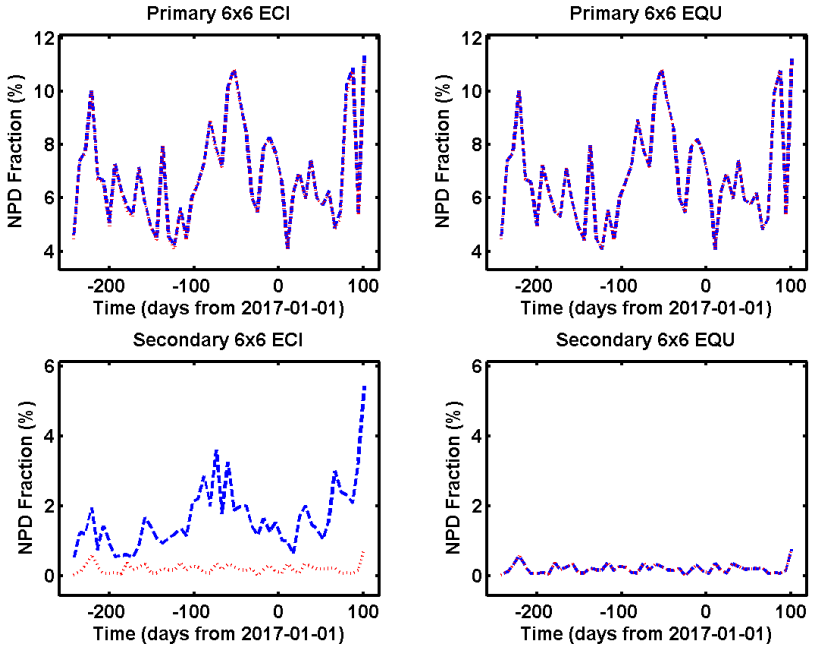

Figure 2. NPD fractions plotted as a function of time during the 11-month study period.

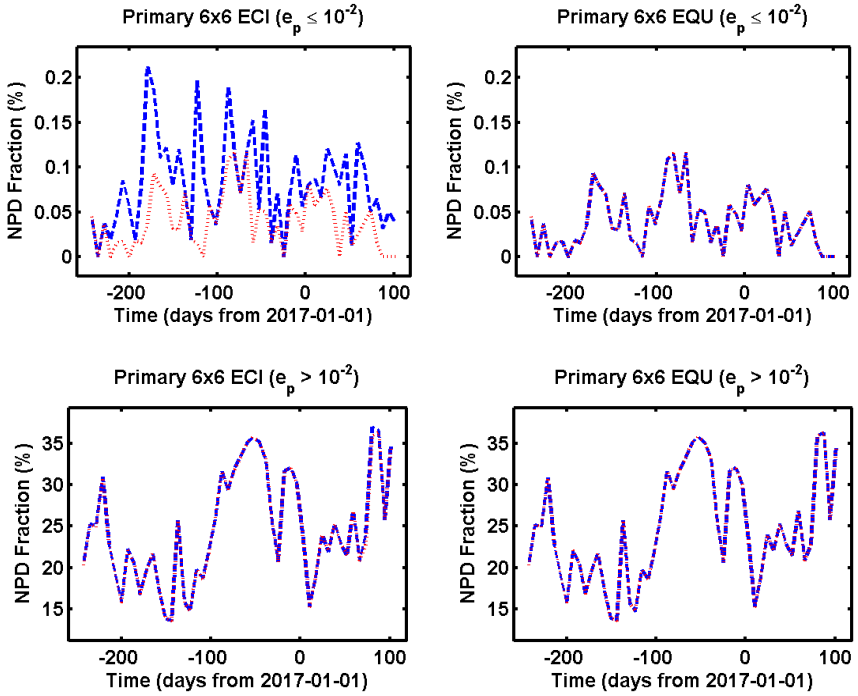

Figure 3. NPD fractions for primaries with low (top) and high eccentricity (bottom).

Empirical Observations from the NPD Analysis

The following observations can be made from the 11-month archive analysis summarized in Table 1 as well as Figures 2 and 3:

1. The 3×3 ECI position covariance and correlation matrices $\{\mathbf{A}_{m,p}, \mathbf{a}_{m,p}, \mathbf{A}_{m,s}, \mathbf{a}_{m,p}, \mathbf{A}_m, \mathbf{a}_m\}$ were found to have significantly fewer NPD occurrences than their 6×6 counterparts. In fact, only one primary — Themis E (SCN 30798), in a highly eccentric orbit with $e_p = 0.83$ — had *any* NPD 3×3 matrices: specifically, in 29 out of its 8,905 conjunctions. All other primaries had 3×3 fractions $F_p = f_p = 0$ exactly. When including all primaries, the NPD fractions $\{F_p, f_p\}$ for the 3×3 matrices were both less than 0.01%, but for the 6×6 matrices both approached 7%. In other words, the NPD frequency for 3×3 matrices could be considered to be negligibly small compared to that of 6×6 matrices. For this reason, the remainder of this section restricts discussion to the 6×6 matrices, unless otherwise stated.
2. NPD fractions for high-eccentricity objects were found to significantly exceed those for low-eccentricity objects (see Figure 3). For example, during the 11-month study period, 23 of the 72 primaries with $e_p < 10^{-2}$ were found to have zero NPD fractions for their ECI covariances, and only three had $F_p > 2\%$. However, the 9 high-eccentricity primaries all had much larger F_p values. Analysis shows that inaccurate interpolation of covariance ephemerides generate a significant portion of these NPD covariances. Specifically, the ephemerides can have relatively large angular spacing near orbital perigee, which degrades the accuracy of the covariance interpolation.
3. Preliminary analysis indicates that primary satellites engaged in maneuvers may also have elevated NPD frequencies, possibly because such objects often require special, customized orbit determination processing. Because many CARA primary satellites regularly maneuver, this may explain some of the elevated NPD fractions observed for low eccentricity primaries.
4. The overall NPD fractions for primary objects typically exceeded those for secondaries by a factor of ~2 or more. This is likely related to the fact that CARA primaries, on average, have higher eccentricities and maneuver more often than the secondaries.
5. Converting ECI state covariances into correlation matrices maintained or reduced the NPD fractions for all objects, i.e., $f_k \le F_k$ for all $k \in \{p,s\}$. The ECI covariances $\{\mathbf{C}_{m,p}, \mathbf{C}_{m,s}, \mathbf{A}_{m,p}, \mathbf{A}_{m,s}\}$ were found to have all positive diagonal elements without exception for the entire data set, allowing calculation of their associated correlation matrices. These ECI covariance→correlation conversions did not ever produce an NPD correlation from a PD covariance, meaning that $b(\mathbf{c}_{m,k}) \le b(\mathbf{C}_{m,k})$ and $b(\mathbf{a}_{m,k}) \le b(\mathbf{A}_{m,k})$ for all $m \in \{1 \ldots M\}$ and $k \in \{p,s\}$.
6. Converting ECI state covariances into equinoctial covariances always maintained or reduced the NPD fractions, i.e., $F_k \le F'_k$ for all $k \in \{p,s\}$. However, 116 (0.03%) and 79 (0.02%) of the equinoctial covariances $\mathbf{C}'_{m,p}$ and $\mathbf{C}'_{m,s}$ were found to have at least one nonpositive diagonal element, respectively, possibly caused by inaccuracies in the ECI→equinoctial transformations, which employed Jacobians approximated using a finite differencing scheme.
7. The NPD status indicators for the entire set of ECI state correlation matrices and equinoctial covariance matrices were found to be identical, and equal to or less than those for the ECI covariances, i.e., $b(\mathbf{c}_{m,k}) = b(\mathbf{C}'_{m,k}) = b(\mathbf{c}'_{m,k}) \le b(\mathbf{C}_{m,k})$ for all $m \in \{1 \ldots M\}$ and $k \in \{p,s\}$. This indicates that the conversions $\mathbf{C}_{m,p} \rightarrow \mathbf{c}_{m,p}$ and $\mathbf{C}_{m,p} \rightarrow \mathbf{C}'_{m,p}$ each had the net effect of maintaining or reducing NPD occurrences. Furthermore, these conversions never created NPD matrices when there was none originally. These NPD status improvements may be related to the better condition numbers of the $\mathbf{c}_{m,p}$ and $\mathbf{C}'_{m,p}$ matrices compared to the $\mathbf{C}_{m,p}$ matrices, as discussed previously.

8. The process of summing the primary and secondary ECI covariances, i.e., $\mathbf{C}_m = \mathbf{C}_{m,s} + \mathbf{C}_{m,p}$ and $\mathbf{A}_m = \mathbf{A}_{m,s} + \mathbf{A}_{m,p}$, did not ever create an NPD combined matrix when there was none originally. Also, the NPD status indicators for the relative state matrices were always less than or equal to the maximum NPD status for the primary or secondary matrices, i.e., $b(\mathbf{C}_m) \le \max[b(\mathbf{C}_{m,p}), b(\mathbf{C}_{m,s})]$, $b(\mathbf{c}_m) \le \max[b(\mathbf{c}_{m,p}), b(\mathbf{c}_{m,s})]$, $b(\mathbf{A}_m) \le \max[b(\mathbf{A}_{m,p}), b(\mathbf{A}_{m,s})]$, $b(\mathbf{a}_m) \le \max[b(\mathbf{a}_{m,p}), b(\mathbf{a}_{m,s})]$ for all $m \in \{1 \ldots M\}$. In fact, the covariance summing process often resulted in a PD combined covariance for conjunctions in which the primary or secondary covariances were NPD, thereby reducing the overall NPD fractions so that $F < \min[F_p, F_s]$ and $f < \min[f_p, f_s]$.
9. Although not shown here, NPD frequencies for covariances expressed in the Cartesian *radial*, *in-track* and *cross-track* (RIC) reference frame[9] (also sometimes called the UVW frame) show qualitatively the same patterns as those expressed in the Cartesian ECI reference frame. In fact, the covariances currently delivered to CARA are expressed in this frame, and were originally produced by interpolating between ephemeris times that bracket the conjunction's TCA (c.f., reference 12).

METHODS OF NPD COVARIANCE REMEDIATION

The CARA system does sometimes encounter conjunctions in which NPD covariances prevent the computation of P_c estimates. For instance, the often-used "2D P_c" approximation[3,4] requires PD status for a marginalized, 2×2 relative position covariance at TCA[3]. Notably, among all of the >800,000 conjunctions analyzed here, only one such NPD 2×2 covariance was found, preventing 2D P_c estimation; this involved a high eccentricity primary with $e_p = 0.68$. CARA's "3D P_c" approximation[13] experiences more frequent NPD issues, because it employs an ephemeris of states and covariances spanning the conjunction, and requires PD relative position covariances, $\mathbf{A}(t)$, at all ephemeris times. Similarly, the relative position Mahalanobis distance at TCA, $M_D(t_{ca})$, which can be used to screen efficiently for negligibly small P_c values,[13] requires PD relative position covariances, $\mathbf{A}(t_{ca})$. Finally, CARA's Monte Carlo P_c estimation algorithm requires equinoctial state covariances with eigenvalues ≥ 0.

When the CARA system encounters such problematic cases, the current approach is to remediate the NPD matrix to a sufficient level that allows the calculation at hand to be performed. Three remediation methods have been investigated for this task: *Spectrum Shifting*, *Higham Remediation*, and *Eigenvalue Clipping*.

Spectrum Shifting Method

Spectrum Shifting entails adding an offset to the entire set or spectrum of matrix eigenvalues, and then constructing a remediated matrix using the original eigenvectors. The first step of this NPD remediation process entails describing an $N \times N$ matrix, $\mathbf{C}$, (which is assumed here to be real and symmetric) using an eigen-decomposition

$$\mathbf{C} = \mathbf{V}\,\mathbf{\Lambda}\,\mathbf{V}^T \tag{3}$$

where $\mathbf{V}$ is a unitary matrix comprising the N orthogonal eigenvectors, and $\mathbf{\Lambda}$ a diagonal matrix of the N associated eigenvalues, $\Lambda_{i,j} = \delta_{i,j}\lambda_i$. In this analysis, eigenvalues are sorted into increasing order so that $\lambda_i \le \lambda_{i+1}$, and associated eigenvectors are denoted $\mathbf{V}_i$. The matrix $\mathbf{C}$ requires no remediation if all of its eigenvalues are positive. If not, the second step defines a shifted set of eigenvalues, γ_i, constructed by adding an offset so all become nonnegative: $\gamma_i = \lambda_i + (|\lambda_{min}| + \varepsilon)$, where $\lambda_{min} = \min[\lambda_i]$ and $\varepsilon \ge 0$. The third step entails using these shifted eigenvalues to construct a remediated matrix

$$\mathbf{C}_{rem} = \mathbf{V}\,\boldsymbol{\Gamma}\,\mathbf{V}^T \tag{4}$$

where $\Gamma_{i,j} = \delta_{i,j}\gamma_i$. For $\varepsilon = 0$, this remediated matrix is PSD by construction, because $\gamma_{min} = 0$ identically. For $\varepsilon > 0$, $\mathbf{C}_{rem}$ is PD by construction with minimum eigenvalue $\gamma_{min} = \varepsilon$. CARA's implementation of the spectrum shifting remediation algorithm employs a default value for ε that is small compared to typical eigenvalues but significantly larger than the computing precision limit. However, ε can be made even larger if needed (for instance, to ensure that Matlab's Cholesky decomposition function *chol* evaluates $\mathbf{C}_{rem}$ as PD, in addition to Matlab's *eig* function).

The principal advantage of the spectrum shifting method is simplicity. One disadvantage is that the method shifts the entire spectrum of eigenvalues upward, even though usually only one of these estimated quantities is originally negative. Another is that the method assumes that the original eigenvectors can be used without modification to construct the remediated matrix in equation (4). A final disadvantage is that there is no objective, physics-based means of establishing what the size of ε should be in cases that require a fully PD remediated covariance.

Higham's Nearest Correlation Matrix Method

Higham Remediation employs methods developed for the financial industry to remediate NPD correlation matrices[6] and covariance matrices[11,14] by finding the closest PSD matrix in terms of Frobenius norm. The CARA software implementation employs the correlation matrix remediation algorithm[6] as the primary method. So when remediating an approximated $N \times N$ covariance matrix, $\mathbf{C}$, the first step of the process entails conversion into the associated correlation matrix, $\mathbf{c}$, using equation (2). As mentioned previously, this requires that the diagonal elements of $\mathbf{C}$ all must be positive to yield a proper, unit-diagonal $\mathbf{c}$ matrix. In the rare cases where any $C_{i,i} \le 0$, Higham's alternate but closely related method[14] is used as the backup algorithm directly for covariance remediation. Given a correlation matrix, $\mathbf{c}$, Higham's algorithm[6] employs nonlinear optimization to estimate the unique PSD matrix with the closest Frobenius matrix norm, $\|\mathbf{c}\|^2 = \Sigma_{i,j}[(c_{i,j})^2]$. The resulting remediated correlation matrix, $\mathbf{c}_{rem}$, is proper in that it has unit-diagonal and nonnegative eigenvalues. The covariance associated with this remediated correlation can be derived by inverting equation (2), $\mathbf{C}_{rem} = \mathbf{D}^{-1}\,\mathbf{c}_{rem}\,\mathbf{D}^{-1}$. The conjunction archive analysis indicates that this method yields $\mathbf{C}_{rem}$ matrices that also usually have nonnegative eigenvalues. However, when that is not the case, then again Higham's alternate method[14] can be used as a backup algorithm.

The principal advantages of the Higham remediation methods are that they have been derived with mathematical rigor, and multiple versions of the implemented algorithms are posted on-line. The disadvantages are that these algorithms are relatively computationally intensive, and designed only to estimate PSD matrices — again leaving unaddressed situations requiring a fully PD remediated matrix. Furthermore, finding the closest matrix in terms of the closest Frobenius norm, while mathematically well defined, is not a physics-based criterion.

Eigenvalue Clipping Method

Eigenvalue Clipping sets a minimum limit for the eigenvalues of a covariance or correlation matrix, and simply forces smaller eigenvalues to this limit. The CARA analysis team developed this method in part to address situations requiring fully PD covariances, such as 3D P_c or Mahalanobis distance estimation. The first step of this remediation process entails eigen-decomposition, as in equation (3). Next, the matrix is deemed to need remediation if any of the eigenvalues are found to be smaller than a nonnegative eigenvalue clipping limit, λ_{clip}, which can be constrained to have a sensible size using physics-based considerations as discussed below. Then, a new set of clipped

eigenvalues can be defined as $\gamma_i = \max[\lambda_i, \lambda_{clip}]$, and the remediated matrix calculated using equation (4). To produce PSD remediated matrices $\lambda_{clip} = 0$; for fully PD remediation $\lambda_{clip} > 0$. When remediating correlation matrices, a final step employing a transformation in the form of equation (2) can be used to ensure that the final result has proper unit diagonal form.

The principal advantages of eigenvalue clipping are that it is the simplest to implement among the three methods, and the physics of hard-body collisions can be used as a basis for remediating position covariances. A disadvantage (shared with spectrum shifting) is that this method assumes that the original eigenvectors can be reused without modification in equation (4).

Eigenvalue Clipping for Marginalized Position Covariances

Physics-based considerations can provide sensible constraints on the eigenvalue clipping limit, λ_{clip}, for marginalized position covariances. This is because the eigenvalues for such covariances can be interpreted[2] as the squares of the 1-sigma widths of the position uncertainty PDFs, specifically $\lambda_i = \sigma_i^2$. For instance, if a primary object has a 3×3 position covariance, $\mathbf{A}_p$, with all positive eigenvalues, then the associated PDF can be visualized as a 1-sigma uncertainty ellipsoid with principal axes aligned with the eigenvectors ($\mathbf{V}_{p,1}$, $\mathbf{V}_{p,2}$, $\mathbf{V}_{p,3}$), and half-width dimensions of ($\sigma_{p,1}$, $\sigma_{p,2}$, $\sigma_{p,3}$). However, if $\mathbf{A}_p$ is PSD with $\lambda_{p,1} = 0$ and $0 < \lambda_{p,2} \le \lambda_{p,3}$, then the PDF becomes confined to a plane, and the 1-sigma surface an elliptical area on that plane. This PSD covariance unrealistically indicates that there is no uncertainty at all in the object's position vector along the direction of the first eigenvector. NPD covariances are even more unrealistic. They lack realism because satellite positions are estimated quantities, based on measurements limited in both number and accuracy, so actual sigma values must always be real and finite. These unrealistic situations occur because $\mathbf{A}_p$ and its eigenvalues suffer from inaccuracies, which can arise a variety of ways as previously discussed.

Eigenvalue clipping constrains the remediated position covariance to have a 1-sigma uncertainty ellipsoid with $\sigma_i \ge (\lambda_{clip})^{1/2}$. One conceivable method of establishing this clipping limit would be simply to impose a limit on how accurate future satellite positions could ever be predicted from the orbital determination estimation process. For instance, detailed analysis and/or long-term experience might allow one to conclude that, for a given set of tracking sensors and measurements, 1-sigma uncertainties on future satellite positions could never be reduced below a lower limit, σ_{lim}. In this case one could sensibly use a clipping limit of $\lambda_{clip} = (\sigma_{lim})^2$. Unfortunately, such σ_{lim} values will likely vary significantly over time and from satellite to satellite; in addition, they may require a prohibitively detailed analysis of the original satellite tracking data to estimate confidently.

Fortunately, considerations based on the physics of collisions can also be used as the basis for covariance remediation in these situations. The P_c estimation process idealizes collisions as occurring when the hard-body radii of the primary and secondary objects begin to overlap as they approach one another.[2,4,5] If any of the primary's estimated eigenvalues are significantly less than the square of its hard-body radius, i.e., $0 \le \lambda_{p,i} << h_p^2$, then random variations in the position vector along the eigenvector direction $\mathbf{V}_{p,i}$ are very small compared to the object size. As explained in more detail below, this means that the probability of collision becomes insensitive to the exact value of $\lambda_{p,i}$, as long as it is significantly smaller than h_p^2. In other words, all eigenvalues satisfying $0 \le \lambda_{p,i} << h_p^2$ should produce approximately the same P_c value. This concept also applies to secondary objects.

To envision this concept, imagine a conjunction with one small primary position eigenvalue, i.e., $0 \le \lambda_{p,1} << h_p^2$, but no other similarly small eigenvalues $\lambda_{p,i}$ or $\lambda_{s,i}$. Next, consider the family of related conjunctions in which $\lambda_{p,1}$ varies over the domain $0 \le \lambda_{p,1} \le h_p^2$, but all other conjunction

parameters remain fixed. Collision probabilities for this family vary with $\lambda_{p,1}$. Let $P_{c,0}$ denote the probability for the family member with $\lambda_{p,1} = 0$. In this case, although there are no random position variations along $\mathbf{V}_{p,1}$, the object itself extends along this direction by $\pm h_p$. For other members of this family with $\lambda_{p,1} << h_p^2$, this situation remains essentially unchanged: the object itself extends along $\mathbf{V}_{p,1}$ by $\pm h_p$ with very small random variations. So these cases should also have collision probabilities approximately equal to $P_{c,0}$. Figure 4 demonstrates this explicitly by plotting 2D P_c values[4] as a function of the ratio $\sigma_{p,1}/h_p$, for the following conjunction TCA parameters (all specified using length units in m, and time units in s): $h_p = 10$, $\mathbf{r}_p = [0\ 0\ 0]^T$, $\mathbf{v}_p = [10^4\ 0\ 0]^T$, $\mathbf{V}_p = [\hat{\mathbf{z}}\ \hat{\mathbf{y}}\ \hat{\mathbf{x}}]$, $\sigma_{p,2} = 20$, $\sigma_{p,3} = 100$, $h_s = 1$, $\mathbf{r}_s = [1\ 0\ 0]^T$, $\mathbf{v}_s = [0\ 10^4\ 0]^T$, $\mathbf{V}_s = [\hat{\mathbf{y}}\ \hat{\mathbf{x}}\ \hat{\mathbf{z}}]$, $\sigma_{s,1} = 20$, $\sigma_{s,2} = 50$, and $\sigma_{s,3} = 200$, where $\hat{\mathbf{x}}$, $\hat{\mathbf{y}}$, and $\hat{\mathbf{z}}$ denote standard unit column vectors. For this notional conjunction, $P_{c,0} = 0.0179$, and P_c values depart from this by less than 0.2% over the range $0 \le \sigma_{p,1}/h_p < 0.1$ (see Figure 4). Analysis indicates that this same pattern holds for many different conjunctions with widely varying encounter geometries, both with fabricated parameters (as in this example), or those taken directly from CARA's archive.

This concept can be exploited for NPD covariance remediation by extending it to the relatively small negative eigenvalues that occasionally occur in conjunction analysis. Again, when the CARA system encounters NPD covariances, most commonly only one of the eigenvalues is negative, and only very slightly so relative to the largest positive eigenvalue. Clipping these slightly negative eigenvalues is appropriate if one assumes they represent estimation inaccuracies (such as interpolation errors), and that a better estimation procedure would have yielded small positive values. CARA's remediation algorithm for 3×3 position covariances employs a clipping limit that corresponds to a small fraction of the object's hard-body radius, i.e., $\lambda_{clip} = (h f_{clip})^2$, with the clipping fraction set to $f_{clip} = 10^{-4}$ by default, although values over the range $10^{-6} \le f_{clip} \le 10^{-2}$ produce essentially equivalent P_c estimates in all cases examined. Relative position covariances, $\mathbf{A} = \mathbf{A}_p + \mathbf{A}_s$, can be remediated using the same approach but using the combined hard-body radius, $h = h_p + h_s$. Notably, this eigenvalue clipping approach produces PD remediated matrices, enabling computation of Mahalanobis distances and 3D P_c values[13] which both require invertible covariances. It also enables 2D P_c computation in the extremely rare conjunctions where the 2×2 marginalized relative position covariance used within that calculation[3,4] is found to be NPD.

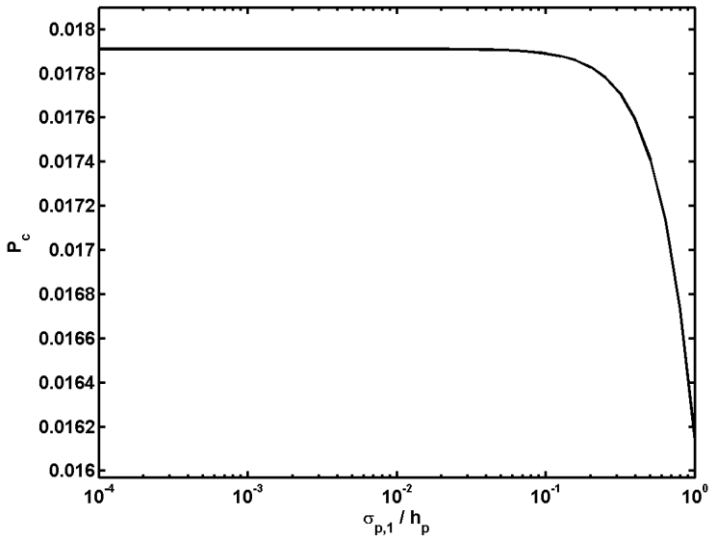

Figure 4. P_c plotted as a function of the smallest primary covariance sigma value.

Eigenvalue Clipping for Monte Carlo Sampling

CARA's Monte Carlo P_c estimation algorithm requires repetitively sampling the equinoctial state probability distribution functions of the primary and secondary objects. Given an object's mean equinoctial state, $\mathbf{x}'$, and covariance, $\mathbf{C}'$, a sampled state, $\mathbf{y}'$, can be written as

$$\mathbf{y}' = \sum_{i=1}^{N} \left[\rho_i \mathbf{V}'_i \sqrt{\lambda'_i} \right] \tag{5}$$

where $\mathbf{V}'_i$ denotes the eigenvectors, λ'_i the eigenvalues, and ρ_i normally-distributed random variates (generated using Matlab's *randn* function). For NPD covariances, this equation will produce sampled states with imaginary values. However, real-valued sampled states can be approximated using an eigenvalue clipping limit of zero, $\lambda_{clip} = 0$, as follows

$$\mathbf{y}' = \sum_{i=1}^{N} \left[\rho_i \mathbf{V}'_i \sqrt{\max[\lambda'_i, 0]} \right] \tag{6}$$

The very slight alteration between equations (5) and (6) indicates how simple the software implementation of eigenvalue clipping can be, especially compared to Higham remediation.

Again, most commonly only one of the NPD covariance eigenvalues is negative, and only slightly so. In these cases, using equation (6) restricts the distribution of sampled states to a five dimensional locus within the six dimensional space of equinoctial states. Similar concepts also apply to sampling Monte Carlo states using the equinoctial state correlation matrix $\mathbf{c}'$ rather than the covariance $\mathbf{C}'$. This approach may have advantages because of the dimensionless nature and better conditioning of the $\mathbf{c}'$ matrices, and is currently being investigated by the CARA team.

EFFECTS OF COVARIANCE REMEDIATION ON COLLISION PROBABILITIES

As mentioned previously, from a purely computational point of view, P_c estimation processes do not always require fully PD state covariance matrices for both of the objects involved in a conjunction. This is especially true for the often-used 2D P_c approximation[3,4] which only requires PD status for a marginalized 2×2 relative position covariance at TCA, regardless of the status of the original state covariances. Of the 830,509 archived events analyzed here, only one conjunction produced such an NPD 2×2 marginalized covariance that prevented the 2D P_c computation. So the vast majority of events that have NPD 6×6 covariances for their TCA primary, secondary and/or relative states can still be processed to provide a 2D P_c estimate without any covariance remediation at all. Even the more demanding 3D P_c computation[13] can be performed in many of these situations without invoking any remediation for similar reasons.

These situations raise concern because of the possibility that the calculated 2D and 3D P_c estimates may be inaccurate because the original covariances were compromised. One way to investigate this possibility is to remediate any NPD 6×6 covariances *before* they are processed for P_c estimation, and then compare the resulting "$P_{c,rem}$" values to the "$P_{c,unrem}$" values calculated without any remediation performed. This study uses the 2D P_c estimation method to perform such a comparison for the 11-month archive data set described above, comprising 428,589 conjunctions with high-precision covariances. When the subset of conjunctions with NPD 6×6 ECI state covariances were remediated using eigenvalue clipping with $\lambda_{clip} = 0$, differences between $P_{c,rem}$ and $P_{c,unrem}$ were all found to be less than 0.2% when restricted to the 2,866 conjunctions with $P_{c,max} = \max[P_{c,rem}, P_{c,unrem}]$ values of 10^{-7} or more. Spectrum shifting remediation produced comparable or

smaller differences. Higham remediation also produced comparable differences, except in one conjunction (out of 2,866) in which $P_{c,rem}$ and $P_{c,unrem}$ differed by about 1.8%. This demonstrates that remediating the full 6×6 ECI covariances before the 2D P_c calculation does not substantially change P_c estimates, regardless of which of the three remediation methods are used. Similar results are also found using the 3D P_c calculation.

Other similar tests could also be performed. For instance, instead of directly remediating any NPD 6×6 ECI state covariances before the P_c calculation, as done above, the covariances could first be converted to equinoctial covariances, remediated in that form, and then converted back into ECI state covariances to be used for the "$P_{c,rem}$" estimates. Similarly, one could first remediate the RIC covariances, followed by RIC→ECI conversions, and then the P_c calculation. Converting to correlation matrices as an intermediate step could also be investigated. However, as mentioned previously, in most cases such remediation is not required from a purely computational point of view. CARA's current approach entails performing remediation only when required by a specific calculation. So to calculate a 2D P_c estimate, remediation would be performed only for the 2×2 marginalized covariance required for that specific calculation (i.e., only once for all of the >800,000 conjunctions analyzed here).

CONCLUSIONS

This analysis indicates that the frequency of NPD 6×6 state covariance matrices in CARA's archive decreased dramatically near 2016-05-01, when the number of CDM significant figures was increased to improve numerical precision. After this time, the fraction of conjunctions involving NPD ECI state covariances for the primary objects decreased to less than 0.1% for low-eccentricity primaries. However, almost 25% of the 6×6 ECI covariances for high-eccentricity primaries were found to be NPD, likely due at least in part to covariance interpolation inaccuracies. The frequency of NPD 3×3 position matrices was significantly smaller than that of 6×6 state matrices.

Converting covariance state matrices to correlation matrices maintains or decreases the frequency of NPD occurrences. Converting Cartesian frame state covariances into equinoctial state covariances similarly decreases NPD occurrences.

Collision probability calculations do not always require fully PD state covariance matrices for both of the objects involved in a conjunction, because these computations often employ marginalized covariances of reduced dimension. Of the >800,000 archived conjunctions analyzed here, only one produced an NPD marginalized 2×2 covariance required for the 2D P_c computation. NPD covariances occasionally need to be remediated when calculating Mahalanobis distances, using the 3D P_c approximation, or when performing Monte Carlo simulations to estimate P_c values. Three methods have been investigated for this task: spectrum shifting, Higham remediation, and eigenvalue clipping. When applied to the archived conjunctions involving NPD ECI state covariances, these three methods produced 2D P_c values that differed only slightly from one another. The eigenvalue clipping method has the advantages of being the simplest among the three, and the only one that provides a means of establishing reasonable, physics-based levels of remediation for NPD position covariances.

ACKNOWLEDGMENTS

The authors would like to thank Joseph Frisbee and Steve Casali for several helpful discussions and analyses, and acknowledge Ron Morgan for the original concept of the spectrum shifting NPD matrix remediation method.

REFERENCES

[1] B.D. Tapley, B.E. Schutz, and G.H. Born, *Statistical Orbit Determination*, Elsevier Academic Press, Burlington, MA, 2004.

[2] P. García, D. Escobar, A. Agueda, and F. Martínez, "Covariance Determination, Propagation and Interpolation Techniques for Space Surveillance," European Space Surveillance Conference, Madrid, Spain, June 7–9, 2011.

[3] K. Chan, *Spacecraft Collision Probability*, El Segundo, CA, The AeroSpace Corporation, 2008.

[4] J.L. Foster and H.S. Estes, "A Parametric Analysis of Orbital Debris Collision Probability and Maneuver Rate for Space Vehicles," NASA/JSC-25898, Aug. 1992.

[5] S. Alfano, "Satellite Conjunction Monte Carlo Analysis," *AAS SpaceFlight Mechanics Meeting*, Pittsburgh, PA, Paper 09-233, Feb. 2009.

[6] N.J. Higham, "Computing the Nearest Correlation Matrix—A Problem from Finance," *IMA Journal of Numerical Analysis* 22, 329-343, 2002.

[7] L.K. Newman and M.D. Hejduk, "NASA Conjunction Assessment Organizational Approach and the Associated Determination of Screening Volume Sizes," *International CA Risk Assessment Workshop*, 19-20 May 2015.

[8] B.L. Livergood, "Implementation of 2014 Screening Volume Analysis," *Flight Dynamics Task Order 21 Technical Memorandum*, FDSS-21-0012, June 2014.

[9] D.A. Vallado, *Fundamentals of Astrodynamics and Applications*, 2rd ed., Microcosm Press, El Segundo CA, 2001.

[10] D.A. Danielson, B. Neta, L.W. Early, *Semianalytic Satellite Theory*, Technical Report NPS-MA-95-002, Monterey, CA, Naval Postgraduate School, 1995.

[11] C. Lucas, *Computing Nearest Covariance and Correlation Matrices*, University of Manchester, School of Mathematics Thesis, 2001.

[12] S. Alfano, "Orbital Covariance Interpolation," *AAS SpaceFlight Mechanics Meeting*, Maui, HI, Paper 04-223, Feb. 2004.

[13] D.T. Hall, M.D. Hejduk, and L.C. Johnson, "Time Dependence of Collision Probabilities During Satellite Conjunctions," *AAS SpaceFlight Mechanics Meeting*, San Antonio, TX, Paper 17-271, Feb. 2017.

[14] N.J. Higham, "Computing a Nearest Positive Semidefinite Matrix," *Linear Algebra and Its Applications*, 103, 103-118, 1988.